B. TECH. PROJECT REPORT

On

Studies on Metamaterials: Application in Civil Engineering

BY

Anshul Srivastava
Ravi Sharma

DISCIPLINE OF CIVIL ENGINEERING
INDIAN INSTITUTE OF TECHNOLOGY INDORE

November 2019

Studies on Metamaterials: Application in Civil Engineering

A PROJECT REPORT

Submitted in partial fulfillment of the requirements for the award of the degrees

of
BACHELOR OF TECHNOLOGY
in
CIVIL ENGINEERING

Submitted by:
Anshul Srivastava
Ravi Sharma

Guided by:
Dr. Saikat Sarkar
(Assistant Professor, Civil Engineering)

INDIAN INSTITUTE OF TECHNOLOGY INDORE
November 2019

<u>CANDIDATE'S DECLARATION</u>

We hereby declare that the project entitled **"Studies on Metamaterials: Application in Civil Engineering"** submitted in partial fulfillment for the award of the degree of Bachelor of Technology in 'Civil Engineering' completed under the supervision of **Dr. Saikat Sarkar, Assistant Professor, Civil Engineering,** IIT Indore is an authentic work.

Further, I/we declare that I/we have not submitted this work for the award of any other degree elsewhere.

Signature and name of the student(s) with date

<u>CERTIFICATE by BTP Guide(s)</u>

It is certified that the above statement made by the students is correct to the best of my/our knowledge.

Signature of BTP Guide(s) with dates and their designation

Preface

This report on "Studies on Metamaterials: Application in Civil Engineering" is prepared under the guidance of Dr. Saikat Sarkar

Through this project, we have explained the concept of metamaterials, basic theory behind creating dispersion and transmission curves and how to interpret them in order to judge the efficacy of the metamaterials. Parametric studies have been performed using different parameter and various applications have been discussed for different models.

There is an extensive use of graphs and figures in the result to vividly describe the observations. We have tried to the best of our abilities and knowledge to explain the content in a lucid manner.

Anshul Srivastava
Ravi Sharma
B.Tech. IV Year
Discipline of Civil Engineering
IIT Indore

Acknowledgements

We wish to thank Dr. Saikat Sarkar for his kind support, expertise and valuable guidance. He provided a perfect environment for critical thinking and research acumen and was always available for discussions, doubt clearance and guidance at every part of the project. He has constantly motivated us to take the project to its very culmination.

We would also like to acknowledge Mr. T. Varma. For his support and sincere cooperation. It is their help and support, due to which we became able to complete the project and technical report.

Without their support this report would not have been possible.

Anshul Srivastava
Ravi Sharma
B.Tech. IV Year
Discipline of Civil Engineering
IIT Indore

Abstract

Some ranges of elastic waves might prove to be hazardous to many civil engineering structures. The use of metamaterial has been an effective way to attenuate waves in optics and acoustics and has also seen a recent advent in mechanics. In this study, different models have been created using the concept of metamaterials for a diverse range of applications.

This project primarily focuses on the study of seismic metamaterials. Initially, the effectiveness of seismic metamaterials is studied by probing the frequency content of an earthquake with and without a metamaterial. Then a different range of bandgaps has been obtained and intrigued by conducting a parametric study on the metamaterial, toying with parameters like shape, size, orientation, and material to optimize the frequency bands in order to manipulate the transmission of elastic ground vibrations. By plotting transmission curves, these results were strengthened as the frequency range of band gaps and transmission loss was observed to be overlapping. Simulations were also performed by fixing the bottom of the inclusions to obtain a range of stop-gap (0 Hz-5 Hz), which is an important aspect.

Effectiveness of metamaterials as engineered defects has been studied in the later part and found to be competent. Such metamaterials can be useful in building components that aim to inundate waves of kHz range. A laminated composite metamaterial has been modeled to be considered for the future aspects of the study.

KEYWORDS: Metamaterial, Microstructure, Bandgap, Stop-Gap, Transmission loss, Defects.

List of Figures

Figure 1: A microscopic photonic metamaterial 2
Figure 2: Array arrangement of microstructures around a building 3
Figure 3: Destruction caused due to an earthquake 4
Figure 4: Propagation of ground vibrations due to railways and metros 4
Figure 5: Direct lattice 6
Figure 6: Reciprocal lattice 6
Figure 7: Unit vector of (a) direct lattice and (b) reciprocal lattice 7
Figure 8: Coordinates of first Brillouin zone 7
Figure 9: Irreducible Brillouin zone 8
Figure 10: Band diagram 8
Figure 11: Periodic arrangement of microstructure: 9
Figure 12: A Typical dispersion curve 10
Figure 13: A typical transmission curve 11
Figure 14: Table of material properties used in the study 12
Figure 15: Zoomed view of an 8-node linear brick element. 12
Figure 16: Node numbering before and after processing the data. 13
Figure 17: Microstructure used to compute frequency content 14
Figure 18: Frequency content of metamaterial 16
Figure 19: Isometric view of a microstructure 17
Figure 20: Results for the cylindrical steel inclusions 17
Figure 21: Results for the hollow cylindrical steel inclusions 18
Figure 22: Results for the hollow square steel inclusions 18
Figure 23: Results for the square steel inclusions 19
Figure 24: Results for the square steel inclusions when rotated by 45^0 20
Figure 25: Comparison of transmission loss at 0^0 and 45^0 orientation 20
Figure 26: Dispersion curve of soil with hollow inclusion showing no bandgap 21
Figure 27: Dispersion curve of soil with concrete inclusion showing no bandgap. 21
Figure 28: Comparison of transmission loss 22
Figure 29: Results for the cylindrical steel inclusions 22

Figure 30: Results for the hollow cylindrical steel inclusions 23
Figure 31: Results for the square steel inclusions 23
Figure 32: Results for the hollow square steel inclusions 24
Figure 33: Results for the hollow defects 25
Figure 34: Results for the steel defects 25
Figure 35: Zoomed view of metamaterial and laminated composites 28

Table of Contents

Candidate's Declaration v

Certificate by BTP Guide(s) v

Preface vii

Acknowledgements ix

Abstract x

List of Figures xi

Table of Contents xii

1 Introduction 1

1.1 Objective: 1

1.2 What are metamaterials? 1

1.3 What is Microstructure? 2

1.4 How can they be effective? 2

1.5 Motivation: 3

1.6 Literature review: 4

2 Background Theory 6

2.1 Solid State Physics: 6

2.1.1 Direct lattice 6

2.1.2 Reciprocal lattice 6

2.1.3 Direct lattice vs Reciprocal lattice: 7

2.1.4 First Brillouin zone: 7

2.1.5 Irreducible Brillouin zone: 7

2.2 Band diagram 8
3 Formation of curves: 9
3.1 Formulation of dispersion curve 9
3.3 Formulation of Transmission Curves: 11
3.3 Data formation 12
4.1 Results and Discussion 14
4.1 Application in Seismic Metamaterials 14
4.1.1 Frequency content 14
4.1.2 Shapes 16
4.1.3 Orientation 19
4.1.4 Materials 21
4.1.5 Stop bandgap (fixed from bottom) 22
5 Conclusion and Future Scope 27
Publications 29
References 30

1 Introduction

1.1 Objective:

Ranging from nanoscale applications in the field of electromagnetic theory, the eminent origin of metamaterials has evolved to large scale implementation as absorbing elastic wave energies, thanks to their diverse architectural characteristics. Our objective is to use this concept on a meter-scale for civil engineering application by doing numerical simulations using different shapes of microstructures in the metamaterial to get an optimum range of bandgaps. A part of the study also focuses on stop bandgap, which is an important aspect in terms of seismic frequencies. The study also aims to analyze another parameter, transmission loss, to evaluate the transfer of energy through the metamaterials. Though this area of research is very naïve, using this concept, a few other innovative applications like the use of metamaterials as defects and as laminated composites have been considered and worked upon.

1.2 What are metamaterials?

There are a lot of engineering properties that are not found in naturally occurring elements; therefore, to achieve them, these materials are engineered accordingly. Such an engineered material is termed as a metamaterial. They are formed from assemblies of multiple microstructures fashioned from composite materials, which in our case is primarily soil with inclusions of materials like steel and concrete. These units are arranged in repeating patterns, at scales that are comparable or smaller than the wavelength they are supposed to influence. Metamaterials do not derive their properties from the base material but their newly designed structures, depending on their material properties, size, shape, geometry, and orientation, etc. This renders it with smart features, making them capable of manipulating elastic waves to achieve the desired benefits that go beyond what is possible with conventional materials.

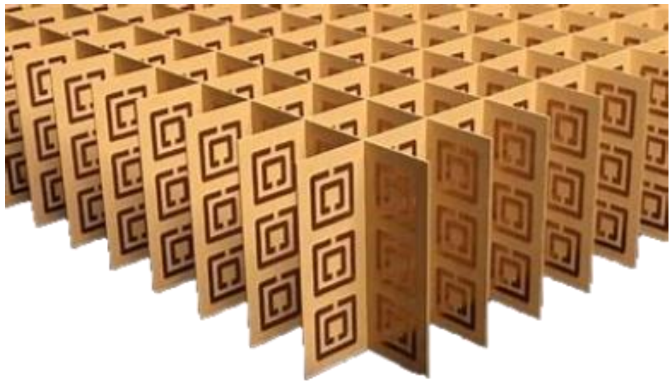

Figure 1: A microscopic photonic metamaterial. *(https://www.smart2zero.com/ n.d.)*

1.3 What is Microstructure?

The smallest recurring element of the metamaterial is termed as its microstructure. By repeating this unit, we can analyze the entire metamaterial. It is the property of this microstructure which is responsible for any behavioral change post-application of metamaterial.

1.4 How can they be effective?

When the frequency of a seismic wave is equal or nearly equal to the natural frequency of the structure, the damage gets amplified. The natural frequencies of most of the buildings lie in the range of 0-6 Hz but there are other important components within as well as outside the structures with various frequencies depending on their sizes. They can be very effective in blocking or at least reducing the frequency content of the hazardous waves passing to a medium and therefore be effective in protecting the structure. Most of the work revolves around creating an array of metamaterials by inclusions in the ground around the structure, whereas later, the work has been steered further to take into account applications in walls, shields and armors etc. by conducting simulations on blocks with defects and laminated composites.

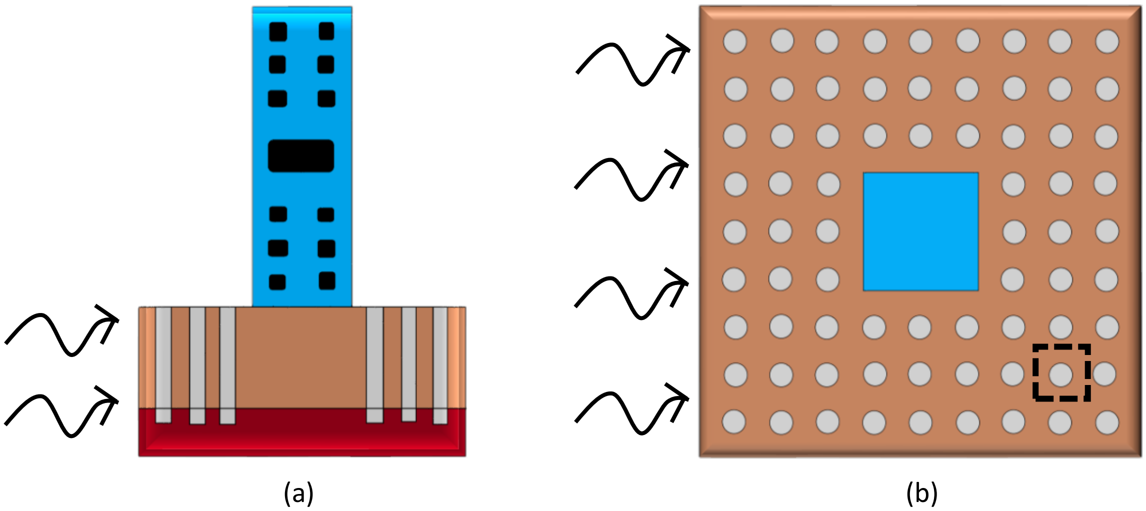

Figure 2: Array arrangement of microstructures around a building: sectional view (a) and plan view (b).

1.5 Motivation:

Millions of earthquakes occur every year in the world. The majority of these earthquakes are of magnitude 2 or lower on the Richter scale, but according to the US Geological Survey, more than 1000 earthquakes occur every year with a magnitude greater than 5. A Tremendous amount of energy is released by the earthquakes which travel in the form of seismic waves. The velocity of seismic waves depends upon the density and elasticity of the material through which it travels. Seismic waves are of two types, namely: body waves (P waves and S waves) and surface waves (Rayleigh waves and Love waves), the latter one being more far-reaching and more destructive. Most of the deaths in earthquakes are due to the collapsing of buildings. Apart from seismic waves, there are numerous other causes of ground vibration like the railways, underground subways, and heavy machinery, etc. which have been causes of destruction in the past. There are many sophisticated structures like some components of Hospitals, petrochemical industries, power plants and nuclear reactors, which cannot afford even the slightest disturbances caused by these waves. These issues have mostly been neglected so far and call for attention as well as viable solutions.

Figure 3: Destruction caused due to an earthquake. *(https://retroexperts.com/ n.d.)*

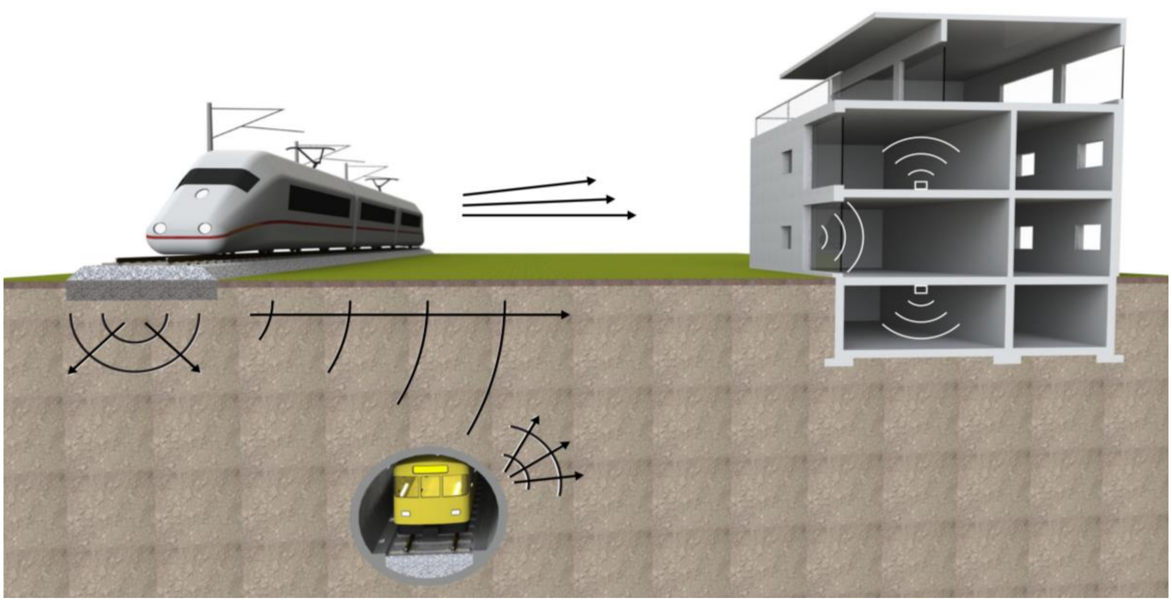

Figure 4: Propagation of ground vibrations due to railways and metros: which can be hazardous to structures over a long period of time. *(http://innorail.hu/ n.d.)*

1.6 Literature review:

To mitigate the impact of earthquake, defense mechanism is required to attenuate the ground vibration and shield the structure from seismic waves. Various techniques have been devised to placate (although meekly) the impacts of earthquakes on structures. A few popular among them are tuned mass damping (TMD) (Kaynia 1981) (Chey 2010) and base isolation (BI) (Skinner 1974)

(Harvey 2016). The natural frequency of a structure cannot be calculated with great accuracy, so the tuning through TMD might not be an easy task in most of the cases. Whereas Base Isolation method is not suitable with soft soil sites and light weight structure (Wagner 2017). Use of seismic metamaterial around the structure is a new approach to attenuate the seismic waves.

One of the first application of metamaterial was done in the field of optics to get some control over the flow of light (Joannopoulos 2008). Studies shows that photonic crystal (electromagnetic metamaterial) can create a bandgap in the emission of light i.e. it is successful in blocking the propagation of a certain range of frequency (John 1987) (Yablonovitch 1987). The use of metamaterials has been done in the field of acoustics where the periodic structure is used to attenuate the sound wave with some frequency range. Inspired from the above studies, researchers have tried to translate the idea to attenuate the waves on a larger scale.

(Hu 2005) showed the refraction of water when waves from the ocean propagate through an array of bottom-mounted vertical cylinders. One of the earliest attempts to attenuate the Rayleigh waves was done in 1999 (Meseguer 1999). In the experiment, cylindrical holes were drilled in a marble quarry and bandgaps were obtained in kHz range, though the range was far higher than required to interfere with seismic ground waves (Meseguer 1999). Another study showed that trees in the forest can naturally act as seismic metamaterials (Colombi 2016). Menard company in France performed an experiment, where an array of vertical empty holes was bored in the soil and a wave source of 50 Hz was used (Brule 2012). Here also the frequency of stop band is higher than required. To attenuate Rayleigh wave and bulk wave in the frequency of 1-10 Hz, (Miniaci 2016) proposed to use hollow, cross-shaped and locally resonant cylinders. However, the limitation of this type of resonant structure lies in obtaining effective stop bands which are large enough for practical use (Achaoui 2017).Early work by Economou and Sigalas (Economou 1993) established a global trait that a denser inclusion material as compared to its host material in the elementary cell of periodic media exhibits bandgaps for 2D and 3D structures. The bandgaps obtained in the process are in the range of kHz which is impractical for seismic applications since high energies contained in seismic activities falls in the range of frequencies of few Hertz only but this might be helpful for this study as it might be used for other applications (Gadallah 2005) (Kramer 2007). First full-scale experiments to shield surface waves, such as Rayleigh waves, were conducted by Brule et. al. (Brule 2012) (SBrule 2017) in structured soil.

2 Background Theory

2.1 Solid State Physics:

2.1.1 Direct lattice

Periodicity of an ideal infinite perfect periodic structure that can be associated to the structure of a finite real crystal is represented by direct lattice.

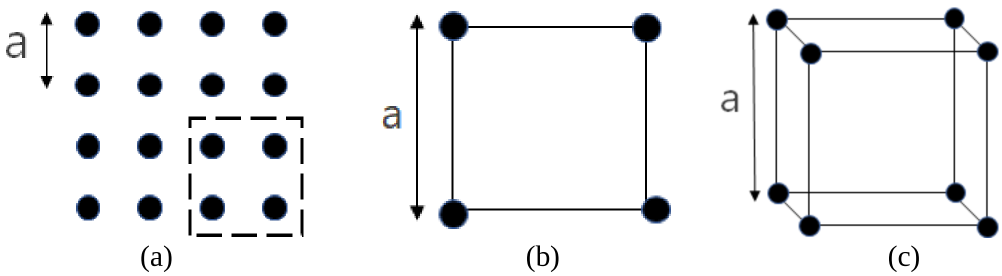

Figure 5: Direct lattice: (a) Representation of periodic matter in 2-D space, (b) unit cell of direct lattice in 2-D space, (c) unit cell of direct lattice in 3-D space

2.1.2 Reciprocal lattice

It is a set of imaginary points, which are obtained by moving in the perpendicular direction to the real space plane with a separation distance equal to the reciprocal of the real interplanar distance. Such points, when arranged in a 3D plane, form the reciprocal space lattice.

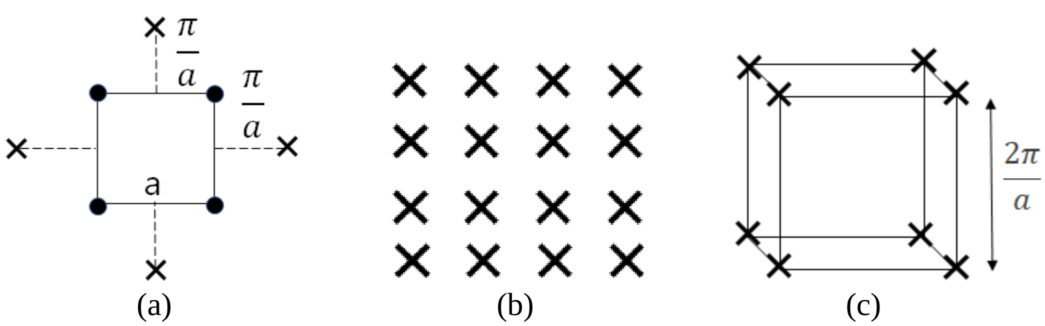

Figure 6: Reciprocal lattice: (a) Location of reciprocal lattice points from unit cell, (b) representation of reciprocal lattice point in 2-D space, (c) unit cell of the reciprocal lattice in 3-D space

2.1.3 Direct lattice vs Reciprocal lattice:

Figure 7: Unit vector of (a) direct lattice and (b) reciprocal lattice

Vectors of the direct lattice are: $\vec{t_1} = a\hat{x} = \begin{bmatrix} a \\ 0 \end{bmatrix}$, $\vec{t_2} = a\hat{y} = \begin{bmatrix} 0 \\ a \end{bmatrix}$

Vectors of the reciprocal lattice are: $\vec{T_1} = \frac{2\pi}{a}\hat{x}$, $\vec{T_2} = \frac{2\pi}{a}\hat{y}$

2.1.4 First Brillouin zone: the brillouin zone is simply the primitive cell in the reciprocal space. Generally, the study of periodic structure is done inside the first brillouin zone.

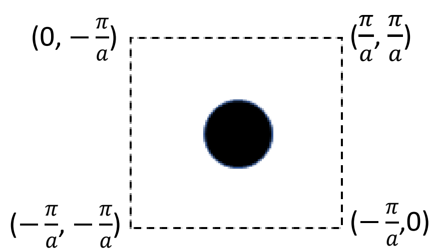

Figure 8: Coordinates of first Brillouin zone

2.1.5 Irreducible Brillouin zone: The Brillouin zone has two planes of symmetry and one 90^0 rotation symmetry. Taking advantage of the symmetricity of the Brillouin zone, the study can be confined in the small area inside the Brillouin zone, known as the irreducible Brillouin zone. The information of the whole first Brillouin zone can be replicated by repeating the information inside the irreducible Brillouin zone.

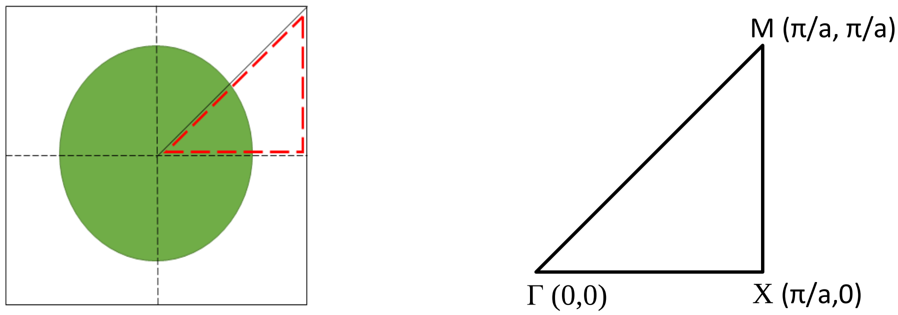

Figure 9: Irreducible Brillouin zone: (a) location of irreducible Brillouin first Brillouin zone, (b) coordinates of irreducible Brillouin zone.

All the critical information of the irreducible Brillouin zone lies on its boundary. This helps us to further confine our study only on the boundary of the irreducible Brillouin zone, not on the whole area inside it. Therefore, knowing the information just on the boundary of the irreducible Brillouin zone, the behavior of the whole first Brillouin zone can be estimated.

2.2 Band diagram

It is a graph of any function (i.e., the function of the wave, example: frequency, energy, etc.) vs. wavenumber, which lies on the boundary of the irreducible Brillouin zone. The x-axis of the graph corresponds to the perimeter of the irreducible Brillouin zone, and the y-axis shows the function. When the function of a wave at y-axis is frequency, the graph is known as the dispersion curve.

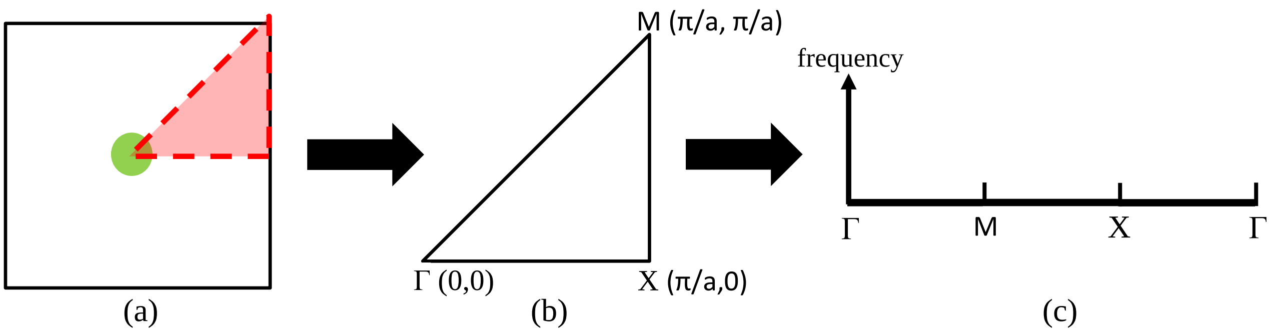

Figure 10: Band diagram: (a) Location of irreducible Brillouin zone in first Brillouin zone, (b) Coordinates of irreducible brillouin zone, (c) Use of irreducible brillouin zone as x-axis in band diagram.

3 Formation of curves:

3.1 Formulation of dispersion curve

Bloch Theorem: Periodic medium or periodic material is defined as the heterogeneity at microstructure level in one, two, or three dimensions. Metamaterial in our study is periodic in X and Y directions.

$$u = \tilde{u}e^{i\left(k_x x + k_y y + k_z z - \omega t\right)}$$

Where,

u = displacement

ω = frequency

$k_x,\ k_y, k_z$ = wave number in x, y and z direction, respectively

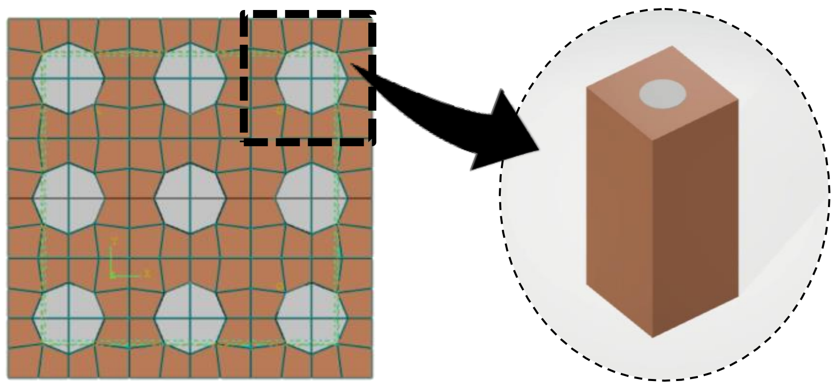

Figure 11: Periodic arrangement of microstructure: Representation of a typical array of microstructures and the repeating structure which is microstructure itself.

Solid Mechanics: For any wave to propagate through elastic medium, it must follow the Navier's equation, which can be written as:

$$(\lambda + \mu)\frac{\partial^2 u_j}{\partial\, x_j\, dx_i} + \frac{\mu \partial^2 u_i}{\partial x_j \partial x_j} = \rho$$

Where,

ρ= density

u= displacement

λ, μ = Lame´'s constant

$$\lambda = \frac{Ev}{(1+v)(1-2v)}, \quad \mu = \frac{E}{2(1+v)}$$

E= modulus of elasticity

v = poison ratio

In this study, for modelling simplicity, all the elements are considered as linearly elastic and isotropic medium, therefore, the properties of waves which propagate through the models are governed by the Navier's equation (equation 1).

Using Bloch Theorem and Navier's equation and discretizing the equation using finite element method, we arrived to the following equation:

$$K\left(k_x, k_y\right) = \omega^2 M(k_x, K_y)$$

Where,

K = stiffness matrix
M = mass matrix
ω = frequency
$k_x,\ k_y$ = wave number in x and y direction.

In the above equation, we can observe that both K (stiffness matrix) and M (mass matrix) are the functions of k_x and k_y, by the sweeping the parameters k_x and k_y along the perimeter of irreducible Brillouin zone (as explained in theory section), we get different values of ω (frequency). (frequency). We can plot the value of at each value of k_x and k_y on the graph, and this graph (frequency vs. wavenumber) is known as the dispersion curve (typical dispersion is shown in Figure 13).

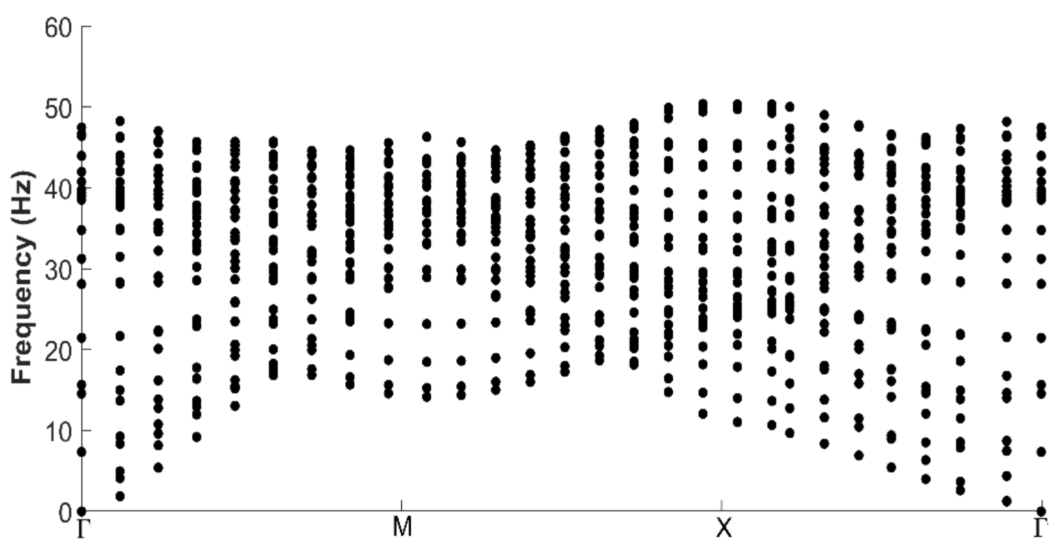

Figure 12: A Typical dispersion curve: having frequency (Hz) on y-axis and wave number on x-axis

3.3 Formulation of Transmission Curves:

Attenuation, also termed as transmission loss, is the gradual loss of flux intensity of a wave while it travels through any material. This is a very common phenomenon used in physics, especially in optics and acoustics, and it is generally measured in decibels (dB).

This study majorly involves ground motions, and attenuation in the energy of signal of ground motion plays a vital role in the assessment of the hazards.

It has been calculated by measuring the acceleration amplitude in the z-direction and using the formula:

$$Attenuation = 10log\ (a2/a1)$$

Where *a1* and *a2* are acceleration amplitudes in z direction at source and destination respectively.

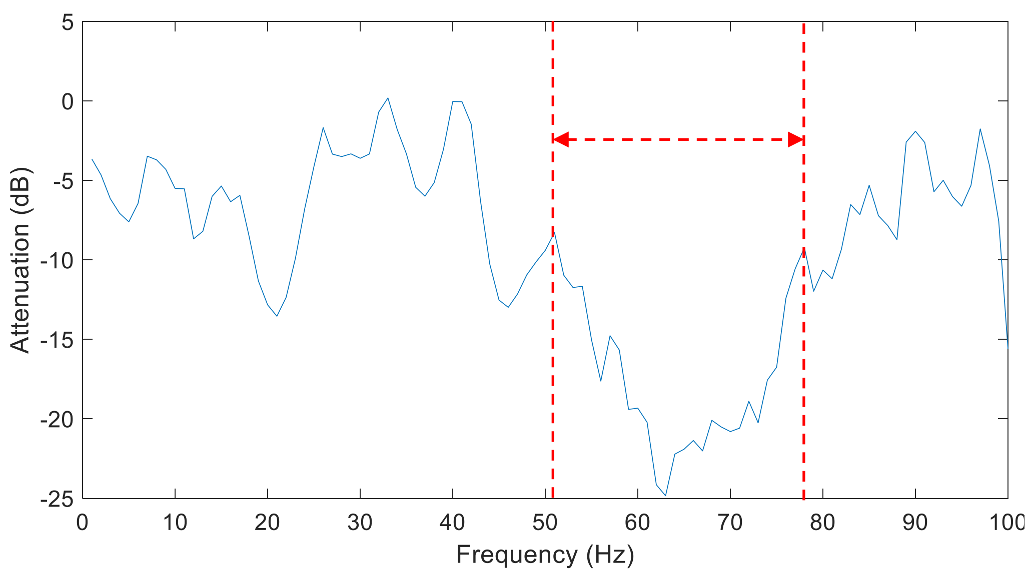

Figure 13: A typical transmission curve: having frequency (Hz) on x-axis and attenuation (dB) on y-axis. The range (from about 50 Hz to 80 Hz) shown within the red dotted lines is the dip in attenuation.

Since dispersion curves are computed over a medium representing an infinite array of elementary cells, they alone do not fully reveal the inherent efficacy of the design. Therefore, the use of a transmission spectrum comes in picture to strengthen the results and give a deeper insight into the effectiveness.

3.3 Data formation

Input: In order to obtain a useable and ordered data to be used for numerical experiments conducted using the above formulation, Abaqus software was used to do modeling of microstructures, which were later repeated by applying Bloch boundary condition. Through numerous steps of modeling, inputs were given in terms of dimensions, material properties, boundary conditions, force, and displacements, etc.

Material	Young's modulus (E) (Pa)	Poisson's Ratio (μ)	Density (ρ) (kg/m^3)
Soil	153×10^6	0.3	1800
Steel	2×10^{11}	0.33	7850
Concrete	22.36×10^9	0.15	2400

Figure 14: Table of material properties used in the study

Meshing Detail: We have used an 8-node linear-brick element (C3D8R) with mesh size of 0.5m.

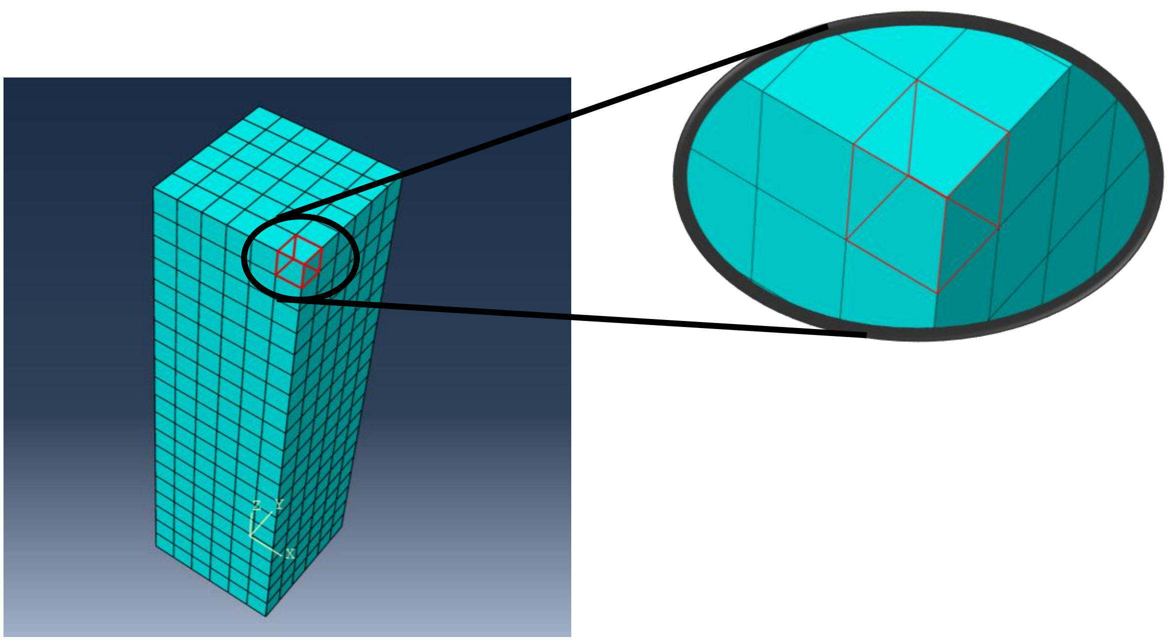

Figure 15: Zoomed view of an 8-node linear brick element.

Outputs:

For calculation of frequency content, earthquake loading was provided at one end, and displacement at the other end was measured.

For the formation of dispersion curve, as we have seen in the mathematical formulation, stiffness matrix and mass matrix were required for which the outputs were obtained in terms of node coordinates, element numbers, and their nodal connectivity.

Acceleration amplitudes on the source and destination points in the Z direction were obtained as outputs to calculate the transmission loss.

Modification and arrangement of data:

After the raw data was obtained, it was modified and arranged according to the needs of the code for the generation of dispersion curve, which was majorly a contribution of Dr. Saikat Sarkar. Few MATLAB codes and functions were contributed for element ordering, combining the mesh data of soil and inclusion material and eliminating common nodes, etc.

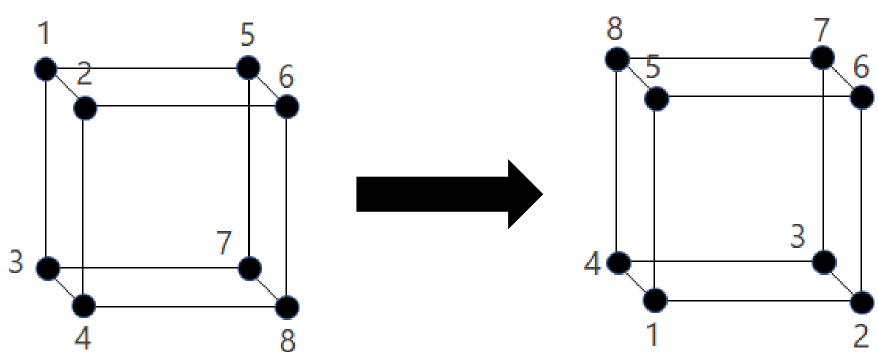

Figure 16: Node numbering before and after processing the data.

4.1 Results and Discussion

4.1 Application in Seismic Metamaterials

4.1.1 Frequency content

To check the effect of microstructure in metamaterial on the waves (at a macro level), we perform a numerical simulation to check the frequency content received when a wave traveled through metamaterial. Two types of microstructures were used in soil (shown in Figure 17), and the results are compared with a soil of the same size without any microstructure.

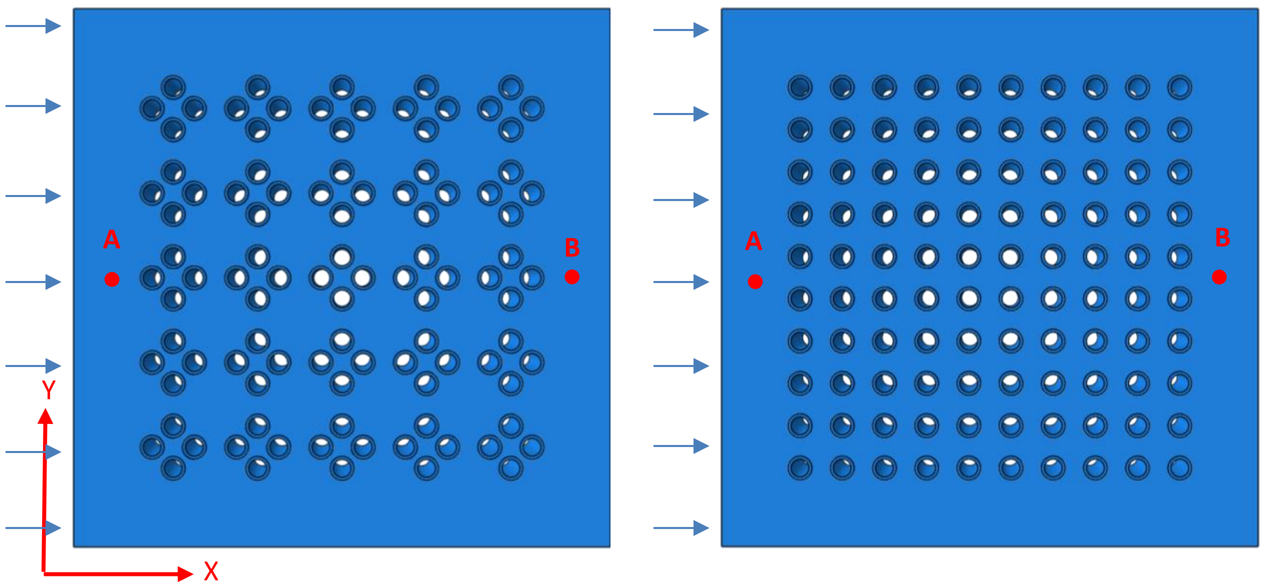

(a) Diamond shaped microstructure (b) Square shaped microstructure

Figure 17: Microstructure used to compute frequency content. Wave is travelling in x direction and observations were taken at point B in both microstructure

The metamaterial used in this seismic analysis consists of soil with a depth of 30 meters and the array of the hollow cylindrical concrete column with an inner and outer radius of 3 and 4 meters respectively. The soil is fixed at the bottom, i.e. no displacements at the bottom layer of soil and the cylindrical concrete column are clamped in the soil. The density of soil and concrete is taken as 1800 kg/m3 and 2500 kg/m3 respectively, the Poisson ratios of concrete and soil being 0.25 and 0.3 respectively and Young's modulus of concrete and soil being 20 GPa and 30 MPa respectively.

The earthquake load was given on the left wall (represented by arrows in Figure 17); therefore, the waves were traveling from point A to point B, i.e., in the x-direction (Figure 17). The displacement of point B was recorded with the help of 'Abaqus' Software, and the frequency content was calculated by applying fast Fourier transform on the displacement data of point 'B' with the help of 'MATLAB'. The frequency content was plotted for all the three cases in x, y and z directions as shown below:

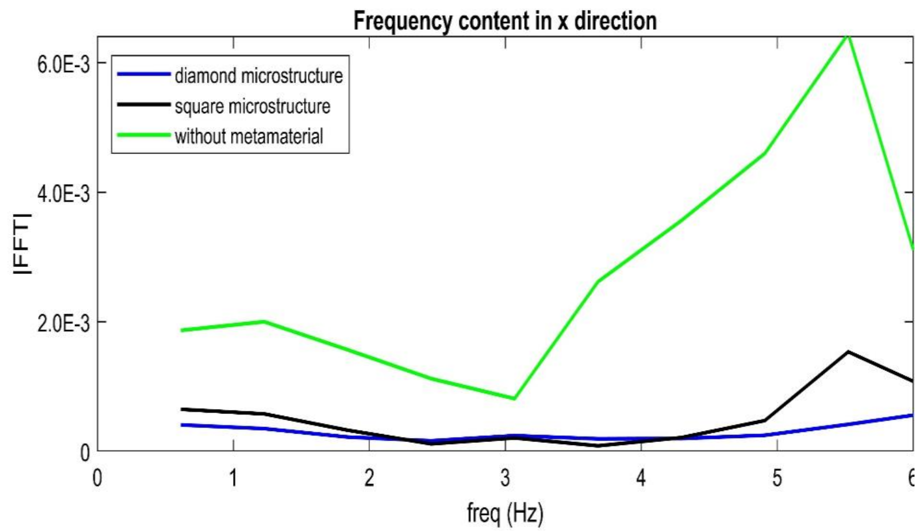

(a)

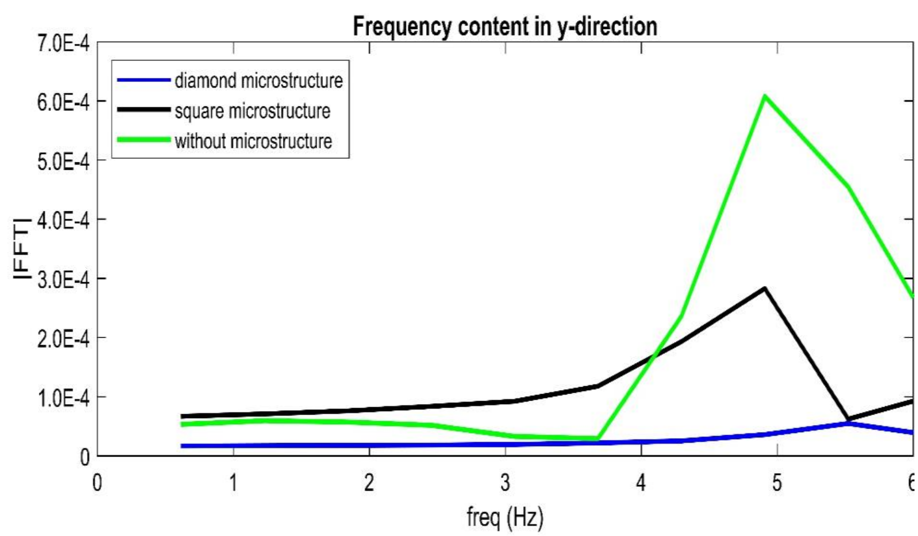

(b)

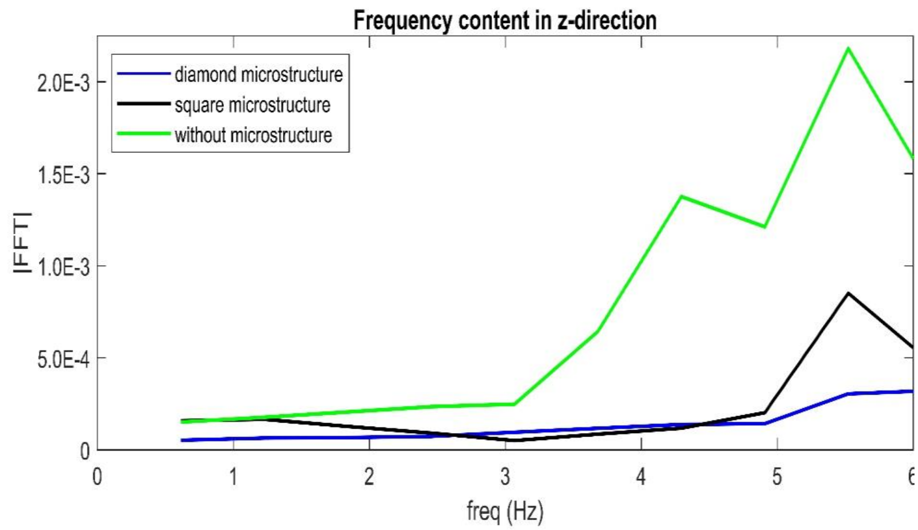

(c)

Figure 18: Frequency content of metamaterial: (a) in x-direction, (b) in y-direction and (c) in z-direction: when the seismic load is applied in diamond microstructure (blue), square (black) microstructure and without microstructure (green)

From the above results, it was concluded that not only the inclusion of metamaterial was effective in reducing the frequency content at the destination point, there were changes observed by changing parameters like the orientation of microstructures. There was a significant decrease in the frequency content after application of metamaterials in x, y, and z directions, and diamond configuration proved to be better than square one, specifically in the higher range of frequencies. This proved the effectiveness of metamaterials and motivated us to take the study further as well as do various parametric studies on them.

4.1.2 Shapes

To study the effects of different shapes of inclusions, numerical simulations were performed with different shapes like circle, square, ring, and frame of equal cross-section areas. Steel inclusion of cross-section area 4 m^2 are taken where density is 7850 Poisson ratio is 0.3, and young's modulus is 200 GPa in the soil of density 1800 kg/m3, poison ratio 0.3 and young's modulus is 153 MPa.

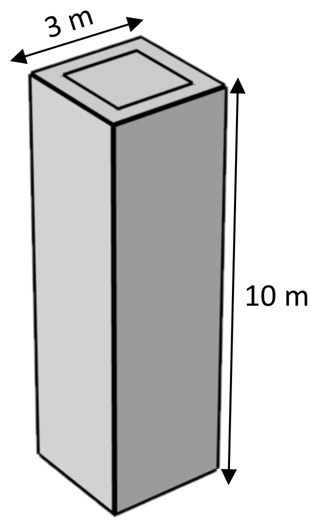

Figure 19: Isometric view of a microstructure

The above figure shows a typical cell that has been used for simulation. By applying Bloch boundary condition on the faces along x and y axis, an infinite array of this structure is being created. All these unit cells are soil columns of square cross sections of 3m x 3m side length and 10m height.

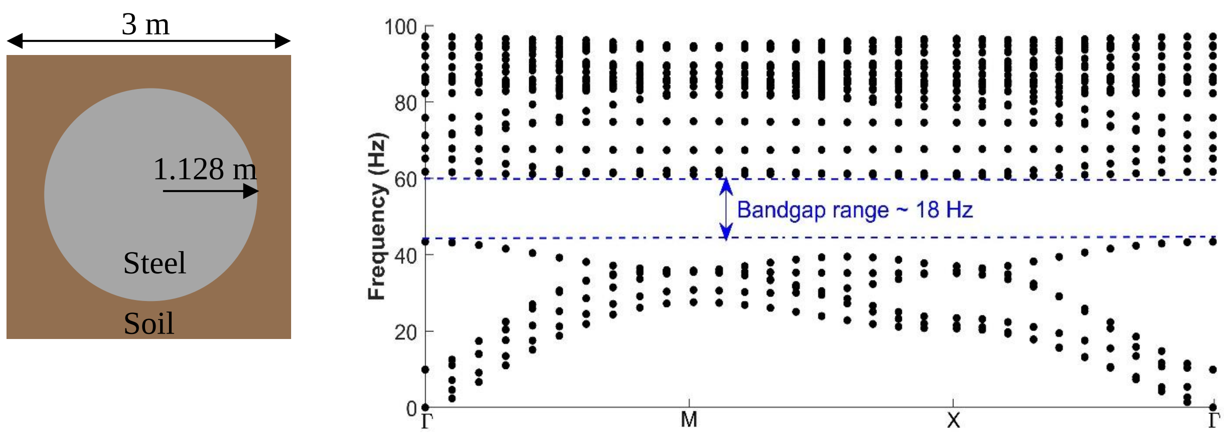

(a) (b)

Figure 20: Results for the cylindrical steel inclusions: (a) Cross-section of microstructure which is steel cylinder of radius 1.128 m and height 10 m embedded in soil (b) dispersion curve showing a band gap of about 18 Hz from 42 Hz to 60 Hz.

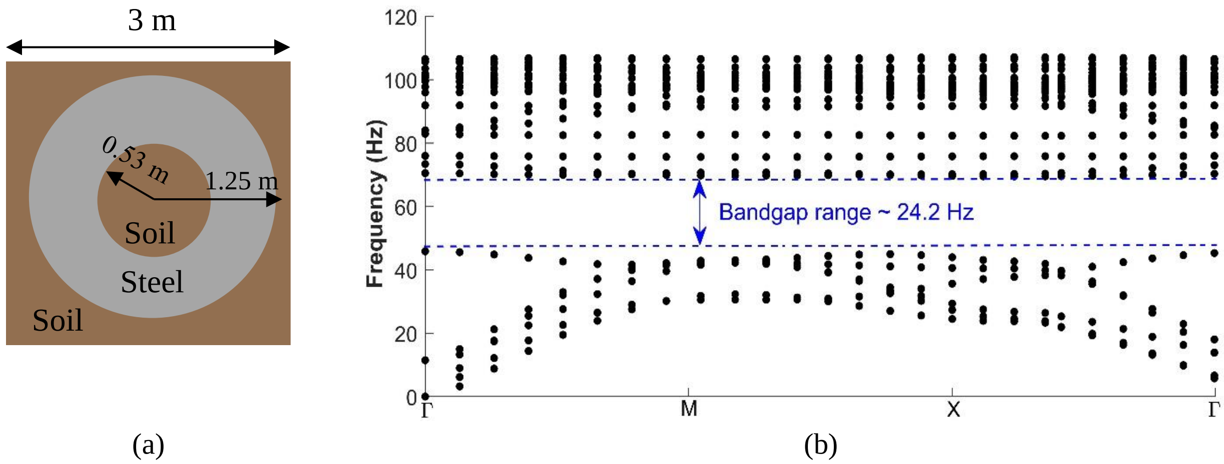

Figure 21: Results for the hollow cylindrical steel inclusions: (a) cross-section of microstructure which is a hollow steel cylinder of outer radius of 1.25 m, inner radius 0.53 m and height 10 m embedded in soil (b) dispersion curve showing a band gap of about 24 Hz from 42 Hz to 66 Hz.

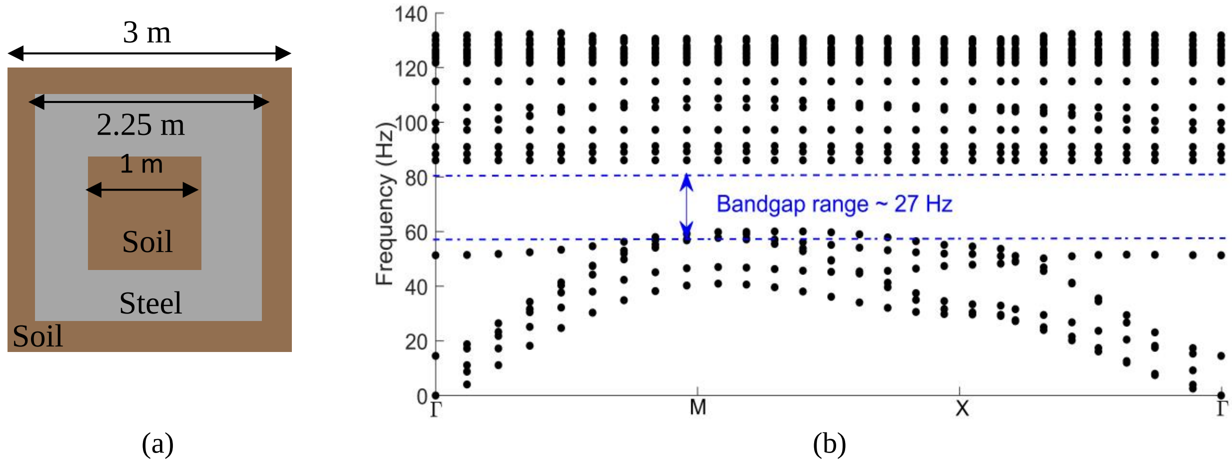

Figure 22: Results for the hollow square steel inclusions: (a) cross-section of microstructure which is hollow steel channel of outer width 2.25 m, inner width 1 m and height 10 m embedded in soil (b) dispersion curve showing a band gap of about 27 Hz from 58 Hz to 85 Hz.

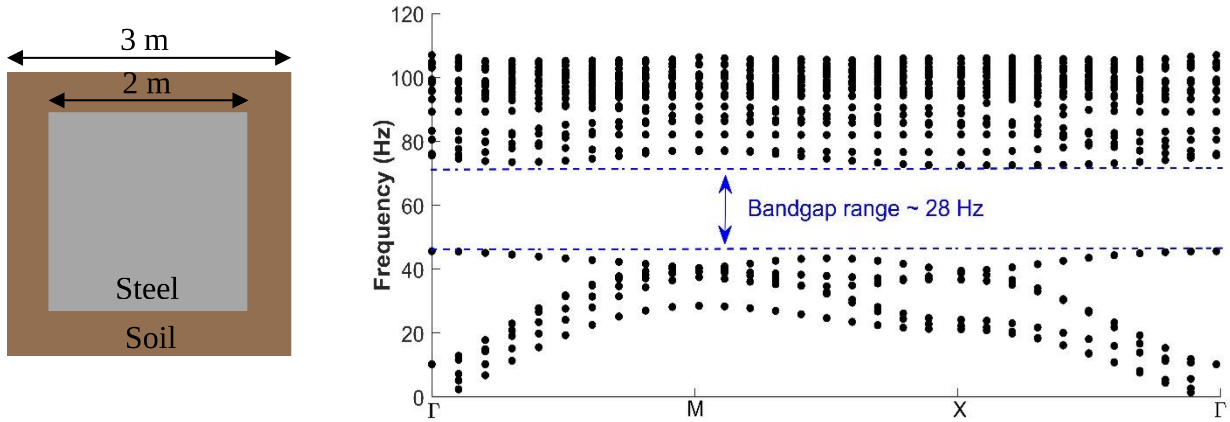

(a) (b)

Figure 23: Results for the square steel inclusions: (a) cross-section of microstructure which is a square steel column of 2 m side length and height 10 m embedded in soil (b) dispersion curve showing a band gap of about 28 Hz from 425Hz to 75 Hz.

From the above dispersion curves (Figure 20-23), we can conclude that there were band gaps observed in all these shapes, but the square cross-section (Figure 23) comes out to be the most preferable one because of the highest range of bandgap. The dispersion curve implies that metamaterial with this microstructure will be able to damp waves lying in the frequency range of about 45 Hz to 75 Hz. Although there can be other complicated shapes with a much higher range of band gaps, for practical purposes, we continued our study with square inclusion.

4.1.3 Orientation

As it was observed that orientation, too, is an important parametric factor which affects the efficiency, to study its impact, simulations were carried out on steel inclusions rotated at an angle of 22.5 degrees and 45 degrees along an axis parallel to the z-axis and passing through the center.

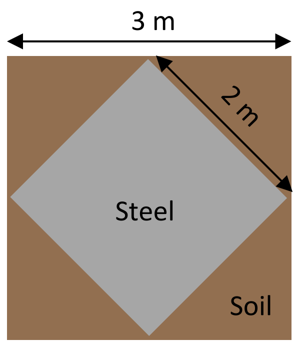

(a)

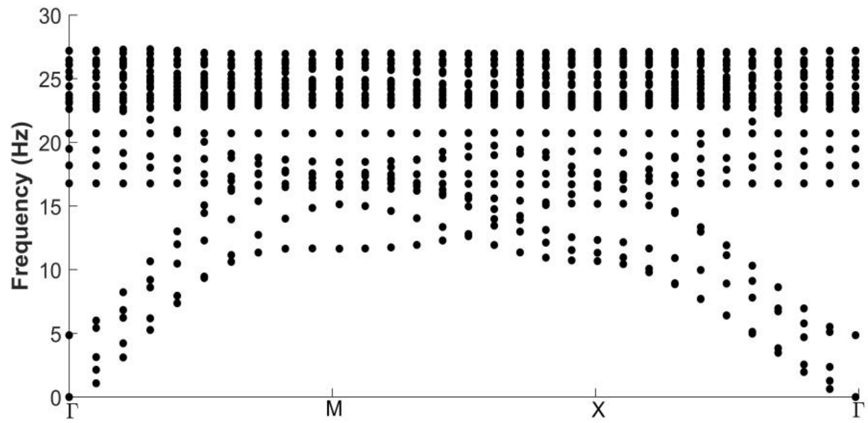

(b)

Figure 24: Results for the square steel inclusions when rotated by 45 degree: (a) cross-section of microstructure which is square steel column of side length 2 m, rotated by 45 degree along the center and height 10 m embedded in soil (b) dispersion curve showing no band gap obtained.

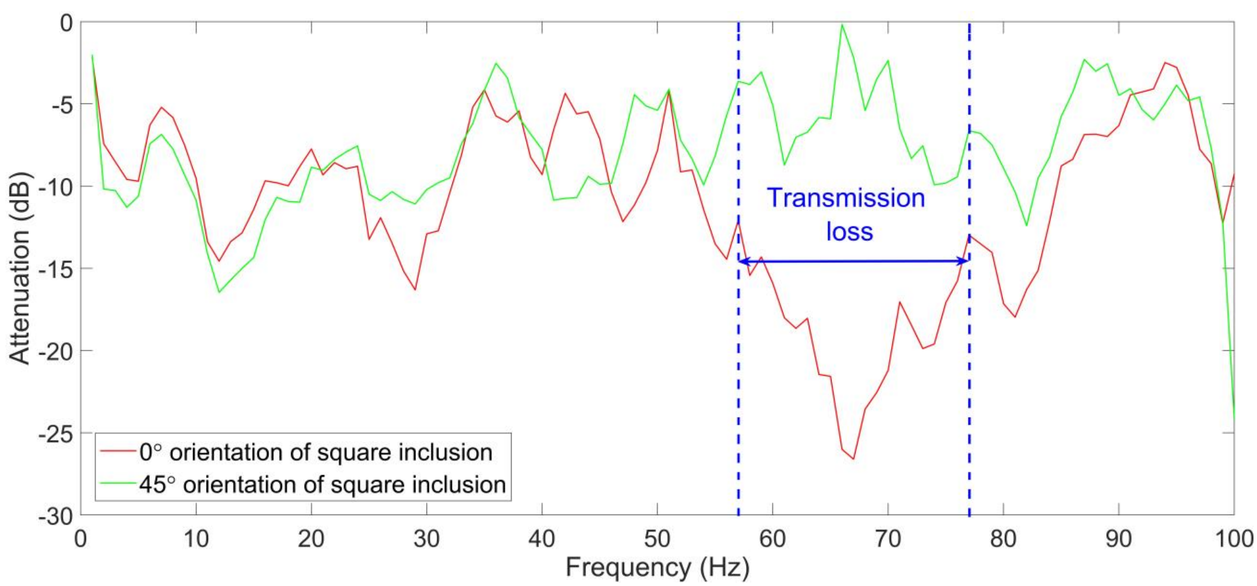

Figure 25: Comparison of transmission loss at 0^0 and 45^0 orientation: showing a clear dip in the bandgap frequency range in the case of 0-degree orientation.

Results show that 0-degree orientation is the best orientation and the bandgap starts decreasing as the angle gets more and more deviated from ideal case.

4.1.4 Materials

Parametric Study on Inclusion material

To study the effects of variation of material properties, a parametric study was performed considering hollow, steel and concrete sections keeping the surrounding soil as the same.

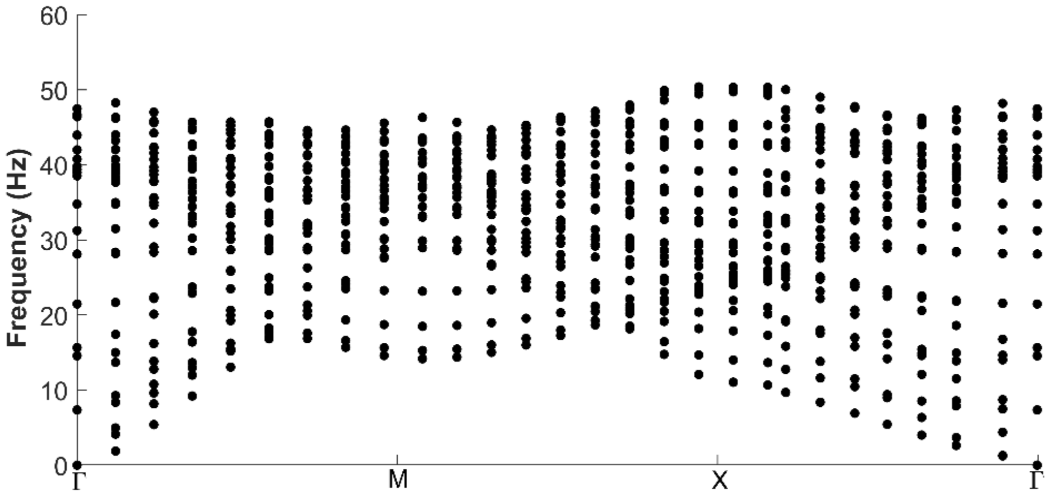

Figure 26: Dispersion curve of soil with hollow inclusion showing no bandgap

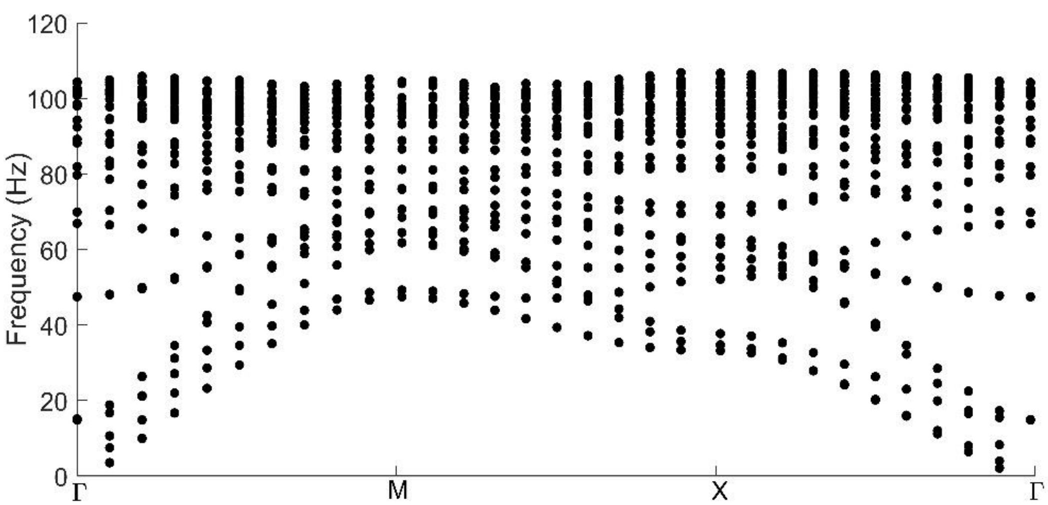

Figure 27: Dispersion curve of soil with concrete inclusion showing no bandgap.

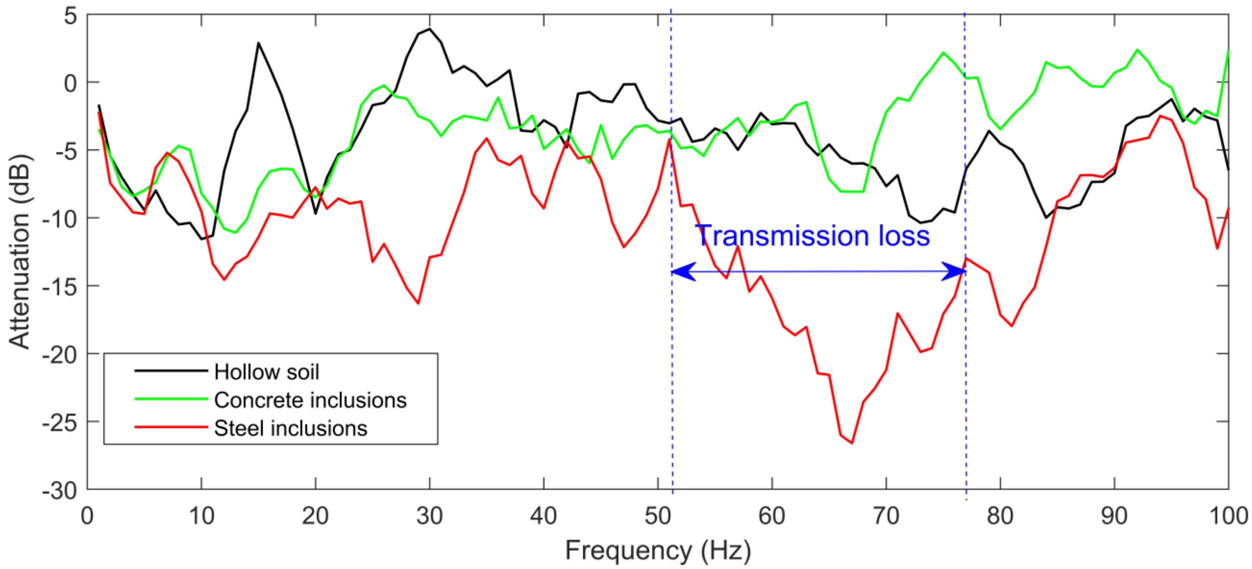

Figure 28: Comparison of transmission loss: of square inclusions with steel (red), concrete (green) and hollow (black)

4.1.5 Stop bandgap (fixed from bottom)

Stop-gap is the lower range of bandgap which is obtained by fixing the lower face of the inclusion. This can be done by reaching the bed rock or clamping the lower part by some other method. This range of bandgap is particularly very useful for protecting building from earthquakes as most of the buildings have their natural frequencies in the range of 0-5 Hz. The upper range however is effective for other components of buildings and its surrounding.

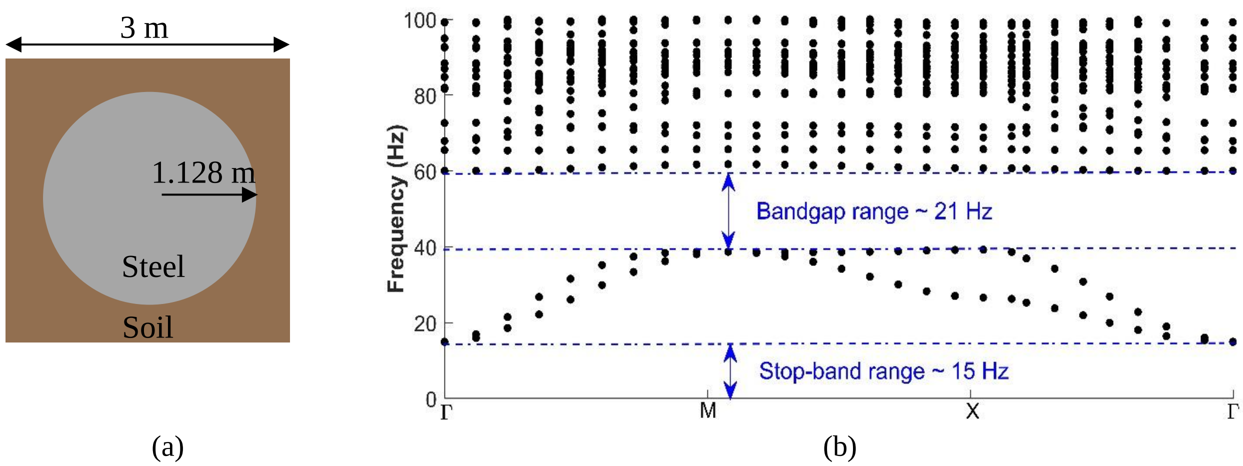

Figure 29: Results for the cylindrical steel inclusions: (a) cross-section of microstructure which is steel cylinder of radius 1.128 m and height 10 m embedded in soil and clamped at bottom (b) dispersion curve showing a bandgap of about 21 Hz and a stop-gap of 15 Hz.

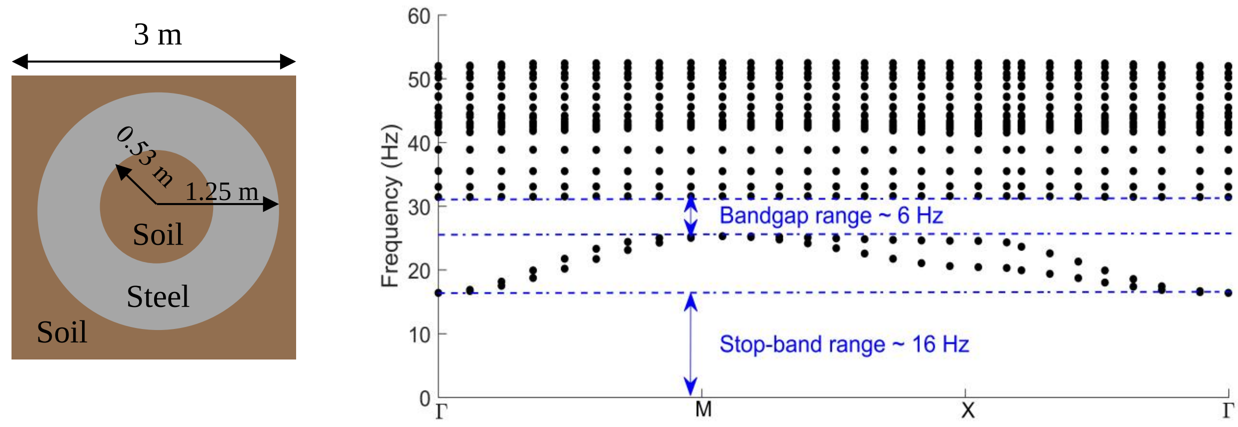

(a) (b)

Figure 30: Results for the hollow cylindrical steel inclusions: (a) cross-section of microstructure which is a hollow steel cylinder of outer radius of 1.25 m, inner radius 0.53 m and height 10 m embedded in soil and clamped at bottom (b) dispersion curve showing a bandgap of 6 Hz and stop-gap 16 Hz.

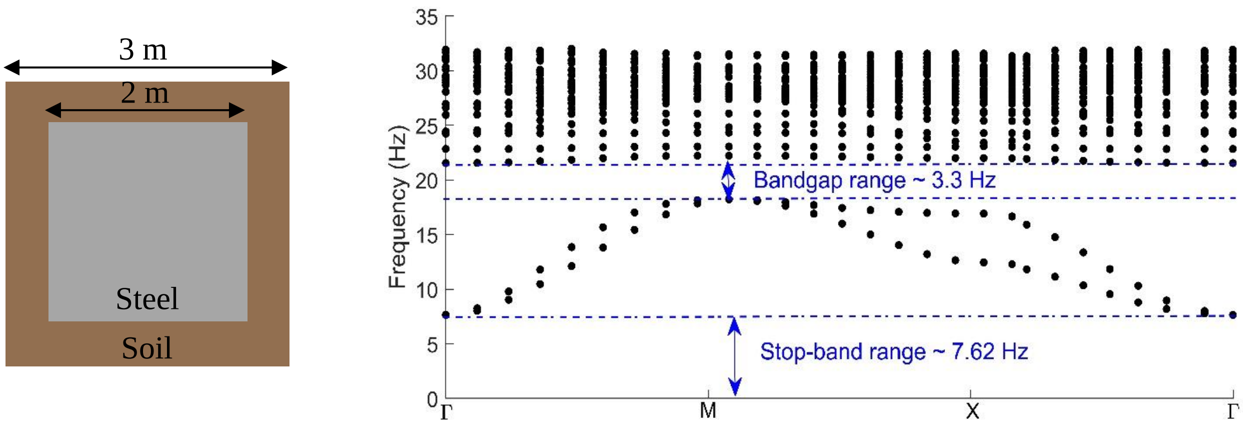

(a) (b)

Figure 31: Results for the square steel inclusions: (a) cross-section of microstructure which is a square steel column of 2 m side length and height 10 m embedded in soil and clamped at bottom (b) dispersion curve showing a bandgap of about 3 Hz and stop-gap of 8 Hz.

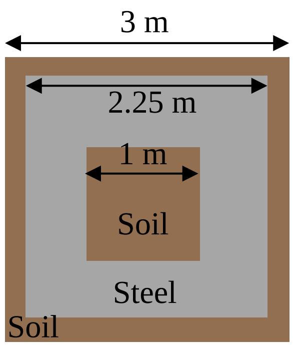

(a)

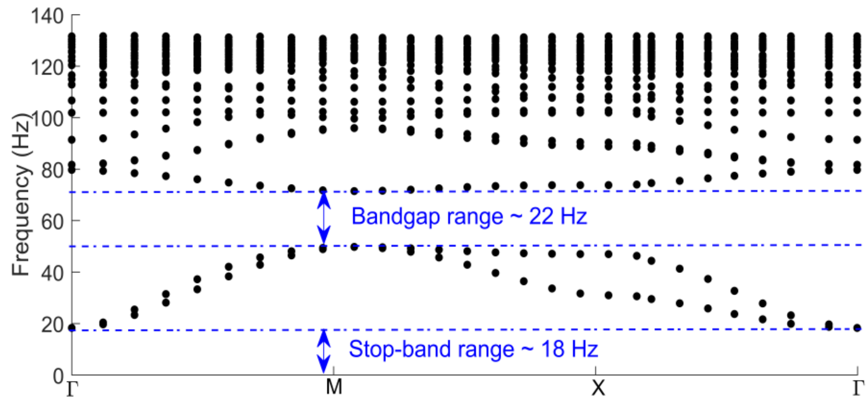

(b)

Figure 32: Results for the hollow square steel inclusions: (a) cross-section of microstructure which is hollow steel channel of outer width 2.25 m, inner width 1 m and height 10 m embedded in soil and clamped at bottom (b) dispersion curve showing a bandgap of about 22 Hz and a stop-gap of 18 Hz.

From the above results (Figure 29-32) it can be observed that we were able to obtain stop-gap range in the lower frequencies by fixing the bottom of the inclusion. The range of band for different geometries varies from 7 Hz to 18 Hz with hollow square steel section showing the highest band of 18 Hz. Therefore, if the focus is only on the stop-gap, then any of the geometries can be considered according to economic and practical feasibility.

4.2 Defects in materials

After successfully analyzing and utilizing the metamaterial for seismic waves, our study has initialized the use of the above mechanism to explore metamaterials as engineered defects. Initially, simulations were performed on soil cubes with hollow spherical defects of different sizes, but it could not result in any bandgap as we can observe in the below figure.

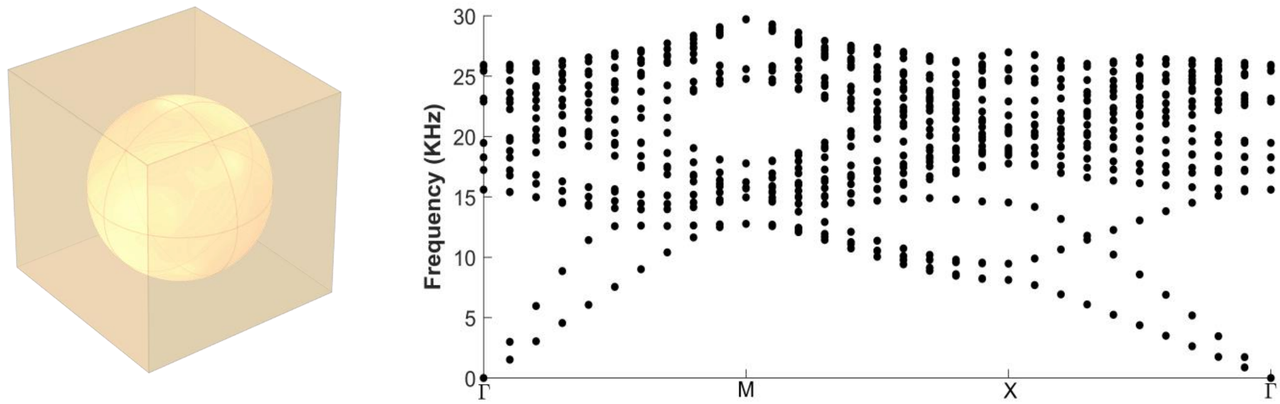

(a) (b)

Figure 33: Results for the hollow defects: (a) 3-D model of a hollow defect in a cube of soil (b) dispersion curve for (a) showing no bandgap obtained.

Further, the study was conducted using defects which are stiffer than the surrounding material. We have taken a steel sphere as a defect in soil. Initially, in the soil cube of 10 mm side length, a spherical steel defect of a 2mm radius was included providing no significant result. But as the radius was gradually increased, a slight bandgap was observed at radius 3.5 mm after with there was a constant increase in the bandgap as the volume (radius) of the defect was increased. A typical dispersion curve for a 4 mm radius spherical steel defect is shown in Figure 35.

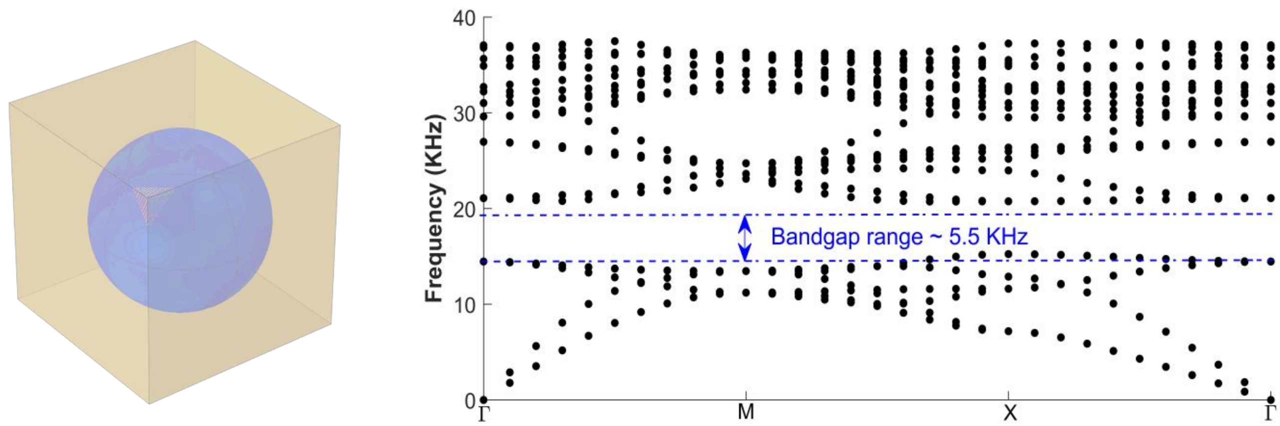

(a) (b)

Figure 34: Results for the steel defects: (a) 3-D model of stiffer (steel) defect in soil cube (b) dispersion curve showing a band gap of approximately 5.5 kHz from about 15 kHz to 20 kHz.

Therefore, we can conclude that using stiffer defects with a volume ratio greater than a minimum amount, which depends on the material properties of the defect as well as surrounding material, a bandgap can be obtained, and waves in a particular frequency can be blocked. We have used a small-sized microstructure to focus on other types vibrations, this arrangement cannot be used as seismic metamaterial but will be useful in applications like making particular walls or flooring for some machinery etc.

5 Conclusion and Future Scope

Therefore, it can be concluded that metamaterials can be effectively used at a meter scale for seismic shielding and for practical civil engineering applications at other scales. Reaching to a reduction in frequency content by simulations, metamaterials were shown to be effective in creating bandgaps in the range of few Hz. Out of the simple geometrical shapes of inclusions, the square was found to be most effective. Though there might be other sophisticated shapes that can prove to be better, for engineering feasibility square was taken. The orientation of microstructure proved to be an essential criterion, and the bandgap completely vanished when the square steel inclusion was rotated by an angle of 45 degrees. Hollow sections and concrete sections could not prove to be effective, which shows that stiffer the inclusion material, better is the bandgap obtained. However, concrete might turn out to be effective when soil properties are changed. These results were strengthened when a dip in transmission curves was observed in the same range as the bandgaps in dispersion curves. If the bottom of the inclusion is fixed, we obtain an interesting range of gaps at the bottom of the dispersion curve termed as a stop-gap. These small bands of a range of about 0 Hz - 5 Hz can be beneficial as the natural frequencies of most of the buildings fall in this realm.

The size of the microstructure determines the range of frequencies where it can prove to be useful since wavelength needs to be comparable to the dimensions of microstructure for proper interaction. Another metamaterial in terms of engineered defect showed promising results. When formed at the millimeter scale, it proved to be effective in the kHz range. These types of engineered defects can be productive in creating walls and floorings of machinery. Metamaterials in the form of laminated composites were modeled and can be a capable study for future aspects having a scope in defense and transportation etc.

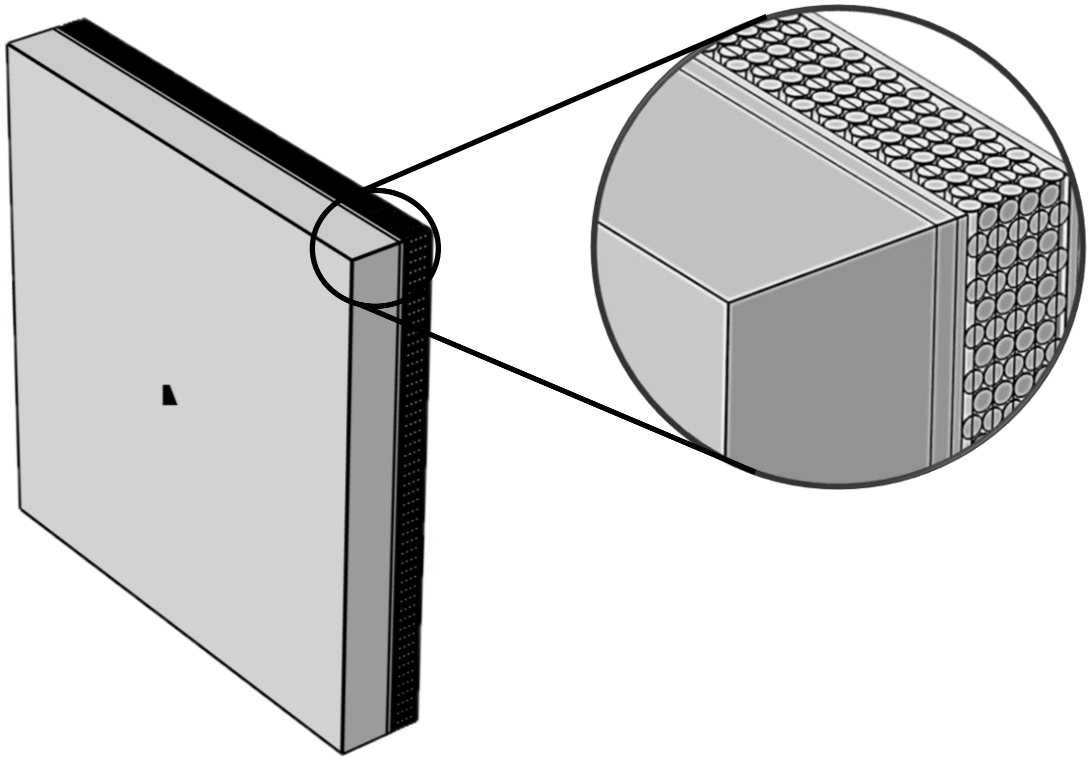

Figure 35: Zoomed view of metamaterial and laminated composites

The model shown in the above figure (Figure 37) is a laminated composite material formed by ceramic (1st layer) and polymer (3rd layer) and joined by an adhesive layer in the middle, where polymer layer is formed as a metamaterial. This is a concept design where the properties of metamaterials can be of great use. Further research can be done on this composite and various applications can be proposed based on this.

Publications

- T. Varma, Ravi Sharma, Anshul Srivastava, Saikat Sarkar, S. Guenneau and R. Craster; Investigation on enhancing bandgap of seismic metamaterials – (Journal paper, to be submitted)

- "Effect of microstructure in seismic metamaterial" – conference paper accepted in ICCMS 2019

References

Achaoui, Y., Antonakakis, T., Brule, S., Craster, R. V., Enoch, S., and Guenneau, S.,. 2017. "Clamped seismic metamaterials: Ultra-low frequency stop bands." *New Journal of Physics* 19 (6): 063022.

Brule, S., Javelaud, E. H., Enoch, S., and Guenneau, S. 2012. "Experiments on seismic metamaterials: molding surface waves." *Physical review letters* 112 (13): 133901.

Chey, M. H., Chase, J. G., Mander, J. B., and Carr, A. J. 2010. "Semi-active tuned mass damper building system: application." *Earthquake Engineering and structural dynamics* 39 (1): 69-89.

Colombi, A., Roux, P., Guenneau, S., Guen, P., and Craster, R.V. 2016. "Forest as a natural seismic metamaterial: releigh wave band gap induced by local resonances." *Scientific reports* 6: 19238.

Economou, E. N., and Sigalas, M. M.,. 1993. "Classical wave propagation in periodic structures: Cermet versus network topology." *Physical review B.* 48 (18): 13434.

Gadallah, M. R., and Fisher, R. L. 2005. *Applied seismology: a comprehensive guide to seismic theory and application.* PennWell Books.

Harvey, P. S., Jr., and Kelly, K. C. 2016. "A review of rolling type seimic isolation: historical development and future directions." *Eng. struct.* 125: 521-531.

n.d. *http://innorail.hu/.* https://www.google.com/url?sa=i&source=images&cd=&cad=rja&uact=8&ved=2ahUKEwj7uaTT74XmAhW47XMBHRzSDPsQjRx6BAgBEAQ&url=%2Furl%3Fsa%3Di%26source%3Dimages%26cd%3D%26ved%3D%26url%3Dhttp%253A%252F%252Finnorail.hu%252Fen%252Fvibration-mitigation-with-under-slee.

n.d. *https://retroexperts.com/.* https://www.google.com/url?sa=i&source=images&cd=&ved=2ahUKEwiPjOa78YXmAhUcUI8KHc03BqsQjRx6BAgBEAQ&url=https%3A%2F%2Fretroexperts.com%2Fbe-prepared-before-during-and-after-an-earthquake-part-1%2F&psig=AOvVaw2QyQBBa6TzHJf_YZQwJHGa&ust=1574789294721634.

n.d. *https://www.smart2zero.com/.* https://www.google.com/url?sa=i&source=images&cd=&ved=2ahUKEwjh2_vY8oXmAhWU4zgGHe3bB_EQjRx6BAgBEAQ&url=https%3A%2F%2Fwww.smart2zero.com%2Fnews%2Fmetamaterials-poised-disrupt-5g-autonomy-and-connected-vehicles&psig=AOvVaw0Twx1HazwHOdHA2hrqBOBt&ust=15747896.

Hu, X., and Chan, C. T. 2005. "Refraction of water waves by periodic cylinder arrays ." *Physical review letters* 95 (15): 154501.

Joannopoulos, J. D., Johnson, S. G., Winn, J. N., and Meade, R. D.,. 2008. "Modeling of flow light." *Princeton Univ. Press, NJ [ua].*

John, S. 1987. "Strong localization of photons in certain diordered dielectric superlattices." *Physical review letters* 58 (23): 2486.

Kaynia, A. M., Biggs, J.M., and Veneziano, D. 1981. "Seismic Effectiveness of Tuned Mass Dampers." *J. Struct. Eng.* 107 (8): 1465-1484.

Kramer, S. L. 2007. *Geotechnical Earthquake Engineering.* Pearson Education, Inc.

Meseguer, F., Holgado, M., Caballero, D., Benaches, N., Sanchez- Dehesa, J., Lopez, C., and Llinares, J. 1999. "Reyleigh-wave attenuation by a semi-infinite two-dimensional elastic-band-gap crystal." *Physical review B* 59 (19): 12169.

Miniaci, M., Krushynsca,A., Bosia, F., and Pugno, N. M. 2016. "Large scale metamaterials as seismic shields." *New journal of physics* 18 (8): 083041.

SBrule, S., Javelaud, E. H., Enoch, S., and Guenneau, S.,. 2017. "Flat lense effect on seismic wave propagation in the subsoil." *Scientific Reports* 7 (1): 18066.

Skinner, R. I., Beck, J. L., and Bycroft, G. N. 1974. "A praticle system for isolating structures from earthquake attack." *Earthquake engineering and structural dynamics* 3 (3): 297-309.

Wagner, P. R., Dertimanis, V. K., Chatzi, E. N., and Bech, J. L. 2017. "Robust-to-uncertainities optimal design of seismic metamaterials." *Journal of Engineering Mechnaics* 144 (3): 040171881.

Yablonovitch, E. 1987. "Inhibited spontaneous immision in solid state physics and electronics." *Physical review letters* 58 (20): 2059.